

Cajal body proteins SMN and Coilin show differential dynamic behaviour in vivo

Judith E. Sleeman, Laura Trinkle-Mulcahy, Alan R. Prescott, Stephen C. Ogg and Angus I. Lamond*

University of Dundee, MSI/WTB Complex, School of Life Sciences, Dow Street, Dundee DD1 5EH, UK

*Author for correspondence (e-mail: a.i.lamond@dundee.ac.uk)

Accepted 29 January 2003

Journal of Cell Science 116, 2039-2050 © 2003 The Company of Biologists Ltd
doi:10.1242/jcs.00400

Summary

Analysis of stable cell lines expressing fluorescently tagged survival of motor neurons protein (SMN) and coilin shows striking differences in their dynamic behaviour, both in the nucleus and during mitosis. Cajal bodies labelled with either FP-SMN or FP-coilin show similar behaviour and frequency of movements. However, fluorescence recovery after photobleaching (FRAP) studies show that SMN returns ~50-fold more slowly to Cajal bodies than does coilin. Time-lapse studies on cells progressing from prophase through to G1 show further differences between

SMN and coilin, both in their localisation in telophase and in the timing of their re-entry into daughter nuclei. The data reveal similarities between Cajal bodies and nucleoli in their behaviour during mitosis. This in vivo study indicates that SMN and coilin interact differentially with Cajal bodies and reveals parallels in the pathway for reassembly of nucleoli and Cajal bodies following mitosis.

Key words: SMN, Coilin, Nucleus, Cajal bodies, Nucleolus, Mitosis

Introduction

The survival of motor neurons protein (SMN) is part of a complex involved in the biogenesis of splicing snRNPs (small nuclear ribonucleoproteins). SMN, together with its associated protein complex, has been widely implicated in the assembly of macromolecular complexes essential for splicing and ribosome biogenesis (reviewed by Terns and Terns, 2001; Gall, 2000; Paushkin et al., 2002) and may also be involved in the biogenesis of the telomerase ribonucleoprotein complex (Bachand et al., 2002). SMN is also proposed to play a direct role in mRNA splicing (Pellizzoni et al., 1998). Mutation of the gene encoding SMN causes spinal muscular atrophy (SMA) (Lefebvre et al., 1997), the leading genetic cause of infant mortality (Pearn, 1980). In SMA, motor neurons degenerate, leading to muscular wasting (Melki, 1997; Talbot and Davies, 2001). The precise way in which a ubiquitously expressed protein with a role in fundamental cellular processes can have such a tissue-specific effect is unclear. It has been proposed that motor neurons may have a particularly high demand for the macromolecules in whose assembly SMN participates (Matera and Frey, 1998). A recent mouse model has shown a correlation between a decrease in the levels of nuclear splicing snRNPs and motorneuron loss in animals expressing low levels of both SMN and its associated protein, *gemin2* (Jablonka et al., 2002).

The nuclear bodies termed gems (gemini of Cajal bodies) are defined by the presence of the protein SMN (Liu and Dreyfuss, 1996). As their name suggests, they are closely related to Cajal bodies (CBs), which are usually defined by the presence of the marker protein p80-coilin (Andrade et al., 1991; Raska et al., 1991). In many cell types, both in vitro and in vivo, the two structures co-localise. CBs and gems appear as different structures, however, in some cell lines and in many

fetal tissues (Matera and Frey, 1998; Young et al., 2000; Sleeman and Lamond, 1999b).

Splicing small nuclear ribonucleoproteins (snRNPs, U1, U2, U4/U6 and U5) are subunits of spliceosomes. They are ribonucleoproteins comprising an snRNA core together with the common, Sm, proteins and several proteins unique to the different snRNPs. Four of the five spliceosomal snRNAs (U1, U2, U4 and U5) are transcribed by RNA polymerase II. Following their transcription they are exported into the cytoplasm where they undergo modification of their 5' termini to form a trimethylguanosine (TMG) cap. The core, Sm, proteins are also assembled in a ring structure around the snRNA (Kambach et al., 1999a; Kambach et al., 1999b). Only once these modifications are complete are the nascent snRNPs re-imported into the nucleus where further maturation occurs before they function in splicing (Fischer et al., 1993; Hamm et al., 1990; Lehmeier et al., 1994; Lerner and Steitz, 1979; Lührmann et al., 1990; Mattaj, 1986; Nagai and Mattaj, 1994; Raker et al., 1996). SMN has a role in the cytoplasmic maturation of snRNPs, most probably in the assembly of the Sm core (Fischer et al., 1997; Pellizzoni et al., 1999; Yong et al., 2002), with a possible additional role in the re-import process (Narayanan et al., 2002; Massenet et al., 2002). Thus, it is probable that the SMN complex is associated with snRNPs throughout the cytoplasmic stages of their biogenesis. Upon re-entry into the nucleus, CBs are the first sites of accumulation of newly assembled snRNPs (Carvalho et al., 1999; Sleeman and Lamond, 1999a), suggesting that the CB may have a function in later stages of snRNP modification or assembly. Furthermore, small nuclear RNAs capable of functioning as guide RNAs for 2'-O-methylation and pseudouridylation have recently been identified as CB components (Darzacq et al., 2002). Studies in cell lines containing separate CBs and gems demonstrate that this putative role in the nuclear maturation of

snRNPs specifically involves CBs that also contain SMN (Sleeman et al., 2001). Thus SMN and coilin may both have roles in nuclear stages of snRNP maturation. Coilin has been implicated as a molecular link, recruiting SMN, its associated proteins and possibly snRNPs into the CB (Hebert et al., 2001).

The presence, in some cell lines, of nuclear bodies containing coilin in the absence of any SMN-complex proteins suggests that coilin-positive bodies and coilin itself may also have other roles within the nucleus. Conversely, the presence of gems containing SMN and its associated proteins in the absence of coilin, suggests that SMN may also have roles independent of coilin. The dynamic behaviour of CBs has been studied in animal and plant cells using a variety of resident proteins as markers, including SmD1 (Sleeman et al., 1998), coilin (Platani et al., 2000; Platani et al., 2002), fibrillarlin (Snaar et al., 2000) and U2B'' (Boudonck et al., 1999). These studies demonstrate that CBs are dynamic structures within nuclei, showing a variety of movements including the joining of CBs, separation of large CBs into smaller CBs and spatial interactions of CBs with each other, with nucleoli and probably also with chromatin. In this study, we have established several cell lines that stably express GFP-SMN and CFP-SMN to examine the dynamics of SMN-positive CBs that will probably be involved in snRNP maturation and to compare the dynamics of the CB proteins SMN and coilin both in interphase cells and through mitosis.

Materials and Methods

Plasmid constructs

pEGFP-SMN has been described previously (Sleeman et al., 2001). pECFP-SMN was generated by sub-cloning the SMN cDNA from pEGFP-SMN into pECFP-C1 (Clontech) using the *BspEI* and *EcoRI* cloning sites in the plasmid multiple cloning site (mcs). To generate pEYFP-coilin, the coilin cDNA was amplified by PCR from plasmid pKH17c (Bohmann et al., 1995). The N-terminal and C-terminal primers contained *BamHI* and *Asp718* restriction sites, respectively. The purified cDNA was then cloned into plasmid pEYFP-C1 (Clontech) using the *BamHI* and *Asp718* sites from the mcs. The structures of the resulting plasmids were confirmed directly by DNA sequencing using an ABI 377 automated sequencer.

Establishment of stable cell lines

Stable cell lines were established using G418 selection of HeLa cells following transfection using Effectene transfection reagent (Qiagen) as described previously (Sleeman et al., 2001).

Cell culture and transfection assays

Cells were grown in Dulbecco's modified Eagles' medium (DMEM) supplemented with 10% fetal calf serum and 100 U/ml penicillin and streptomycin (Life Technologies). Medium used to maintain stable cell lines also contained 200 µg/ml G418 (Life Technologies). For immunofluorescence assays, cells were grown on coverslips and transfected (if necessary) using Effectene transfection reagent (Qiagen) according to the manufacturer's instructions. For the preparation of cell lysates, cells were grown in 10-cm diameter dishes. For live cell microscopy, cells were grown on 32 mm coverslips (Intracel).

Cell fixation and immunostaining

Cells were grown on glass coverslips and fixed for 10 minutes in 3.7%

paraformaldehyde in 37°C PHEM buffer (60 mM PIPES, 25 mM HEPES, 10 mM EGTA, 2 mM MgCl₂, pH 6.9). Following a 10-minute permeabilisation with 1% Triton X-100 in phosphate-buffered saline (PBS), cells were blocked with 1% donkey serum for 10 minutes and then incubated with primary antibodies for 30 minutes, washed, and incubated with secondary antibodies (Jackson Labs) for 30 minutes. If required, cells were stained with DAPI (0.3 µg/ml; Sigma). After a final set of washes, cells were mounted in Vectashield medium (Vector Labs). Primary antibodies used were Y12 anti-Sm (Pettersson et al., 1984), 204 anti-coilin (Bohmann et al., 1995), MANSIPI anti-SIP1/Gemin2 (a gift from G. Morris) and Ab1 anti-TMG (Calbiochem).

Preparation of cell lysates, immunoblotting and immunoprecipitation

Cells were washed twice with ice-cold PBS and then lysed in 0.5 ml of ice-cold 50 mM Tris-HCl pH 7.5; 0.5 M NaCl; 1% (v/v) Nonidet P-40; 1% (w/v) sodium deoxycholate; 0.1% (w/v) SDS; 2 mM EDTA plus Complete protease inhibitor cocktail (Roche, one tablet per 25 ml). The lysate was passed through a Qiasredder column (Qiagen) to break up the DNA and then cleared by centrifugation for 15 minutes at 4°C and 13,000 rpm. Lysates were electrophoresed on an 8% SDS-polyacrylamide gel and transferred to nitro-cellulose membranes for immunoblotting. Immunoprecipitation using anti-green fluorescent protein (GFP) antibodies (Roche) was performed as described previously (Trinkle-Mulcahy et al., 2001). Primary antibodies used were anti-GFP mouse monoclonal (Roche), MANSMA1 anti-SMN (Young et al., 2000) and MANSIPI anti-Gemin2/SIP1 (a gift from G. Morris).

FACS analysis

Cells were harvested by trypsinisation and fixed in 70% ethanol for 3 hours at 4°C. Cells were stained with propidium iodide (25 µg/ml) containing RNase A (100 µg/ml). Fluorescence was measured using a FACScan (Becton Dickinson). Data analysis was performed using Cell Quest software (Becton Dickinson).

Microscopy of fixed cells

Immunostained specimens were examined using a Zeiss 100× NA 1.4 PlanApo objective. Images were recorded on a Zeiss DeltaVision Restoration microscope (Applied Precision) equipped with a 3D motorised stage and a Roper Scientific Micromax camera containing a Sony Interline 1300 CCD. For each cell, optical sections separated by 200 nm were recorded using a binning of 2×2. Images were restored using a constrained iterative deconvolution algorithm using an empirically measured point-spread function.

Microscopy of live cells

For live cell microscopy, cells were grown on glass coverslips and mounted in phenol-red free medium in a closed, heated chamber (Biopetechs FCS2). Imaging and restoration were performed essentially as for fixed cells, but using a 500 nm separation of optical sections. Time points were taken between 3 minutes and 5 minutes apart.

Photobleaching analyses

Short time-course fluorescence recovery after photobleaching (FRAP) analyses were performed using a Zeiss 510 confocal laser scanning microscope equipped with an argon-krypton laser. Cells were maintained at 37°C in a closed chamber (Helmut Saur POC). Using a 63×, 1.4NA PlanApo lens (Zeiss) and the 488 nm laser line, image acquisition was performed using 10% of laser power. Photobleaching was performed using 80% of laser power and 100 iterations.

Following bleaching, images were collected at 4- or 5-second intervals using 10% laser power. A pinhole setting of 1.32 Airy units was used for image collection. Quantitation was performed using the LSM510 software. Long time-course FRAP analyses were performed using a Zeiss 410 confocal laser scanning microscope. A series of optical sections were taken using a 488 nm laser at 1/30 of full power. Bleaching was performed using the laser at full power, using 6 iterations, each with a dwell time of 0.24 milliseconds per pixel. Z-series of images were then collected at 5-minute intervals using 1/30 of laser power. Fluorescence loss in photobleaching (FLIP) analyses were performed using bleaching settings as above, with series of images collected before the initial bleach and after each bleaching event. Quantitation was performed using SoftWorx software (Applied Precision) as previously described (Sleeman et al., 2001).

Results

Characterisation of GFP-SMN and CFP-SMN cell lines

Stable HeLa cell lines were established expressing either GFP-SMN (lines GFP-SMNE18.6 and GFP-SMNE10.3) or CFP-SMN (lines CFP-SMNE12A and CFP-SMNE8.8), using G418 selection of transiently transfected cells (see Materials and Methods) (see Sleeman et al., 2001). In each cell line, FP-tagged SMN is expressed in >95% of cells. The tagged proteins give a localisation pattern of diffuse cytoplasmic staining and a small number of intense nuclear bodies when analysed by

fluorescence microscopy (Fig. 1). This is identical to the localisation pattern of endogenous SMN in the parental HeLa cell line as shown by immunofluorescence (data not shown) (see Sleeman and Lamond, 1999b). The GFP-SMN nuclear bodies co-localise with Sm proteins (Fig. 1A,C), the CB marker coilin (Fig. 1D,F) and the SMN-complex protein SIP1/Gemin2 (Fig. 1G and I). Again, this is identical to the localisation seen for each of these factors in the parental cell line (data not shown). Furthermore, no change in the morphology of other nuclear structures, including speckles (Fig. 1A,C) and nucleoli (data not shown), is apparent upon constitutive expression of FP-SMN.

We analysed the expression levels of the tagged proteins in the stable cell lines. Lysates of total protein from cell lines CFP-SMNE8.8 (Fig. 2A) and GFP-SMNE18.6 (data not shown) were separated by SDS PAGE, transferred to nitrocellulose and probed with anti-SMN and anti-FP antibodies (see Materials and Methods). Both antibodies show a single band of the expected size for FP-SMN (68 kDa). Detection with anti-SMN antibodies shows a second band, representing endogenous SMN (38 kDa), and demonstrates that CFP-SMN is expressed at a lower level than endogenous SMN (Fig. 2A, left-hand panel). Similar analysis of total protein lysates from the parental HeLa cell line and from HeLa cells transiently transfected with a plasmid expressing CFP alone show a single band representing

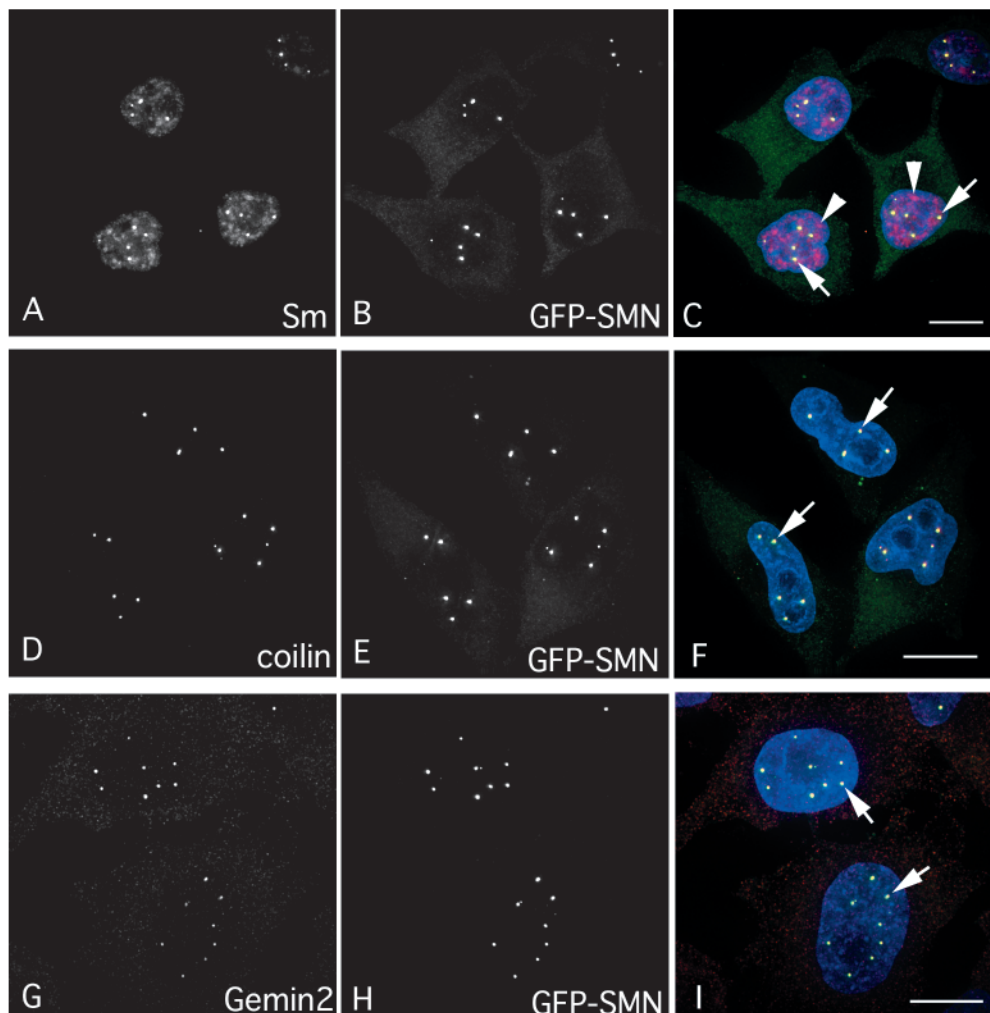


Fig. 1. Stable cell lines expressing GFP-SMN show normal nuclear morphology. Three-dimensional serial sections of deconvolved serial sections showing cells from line GFP-SMNE10.3 (green) counterstained with antibodies to Sm proteins (A-C), coilin (D-F) and SIP1/Gemin2 (G-I). GFP-SMN co-localises in Cajal bodies with Sm proteins (arrows in C), coilin (arrows in F) and SIP1/Gemin2 (arrows in I). Sm-containing speckles are also visible (arrowheads in C). Bar, 10 μ m.

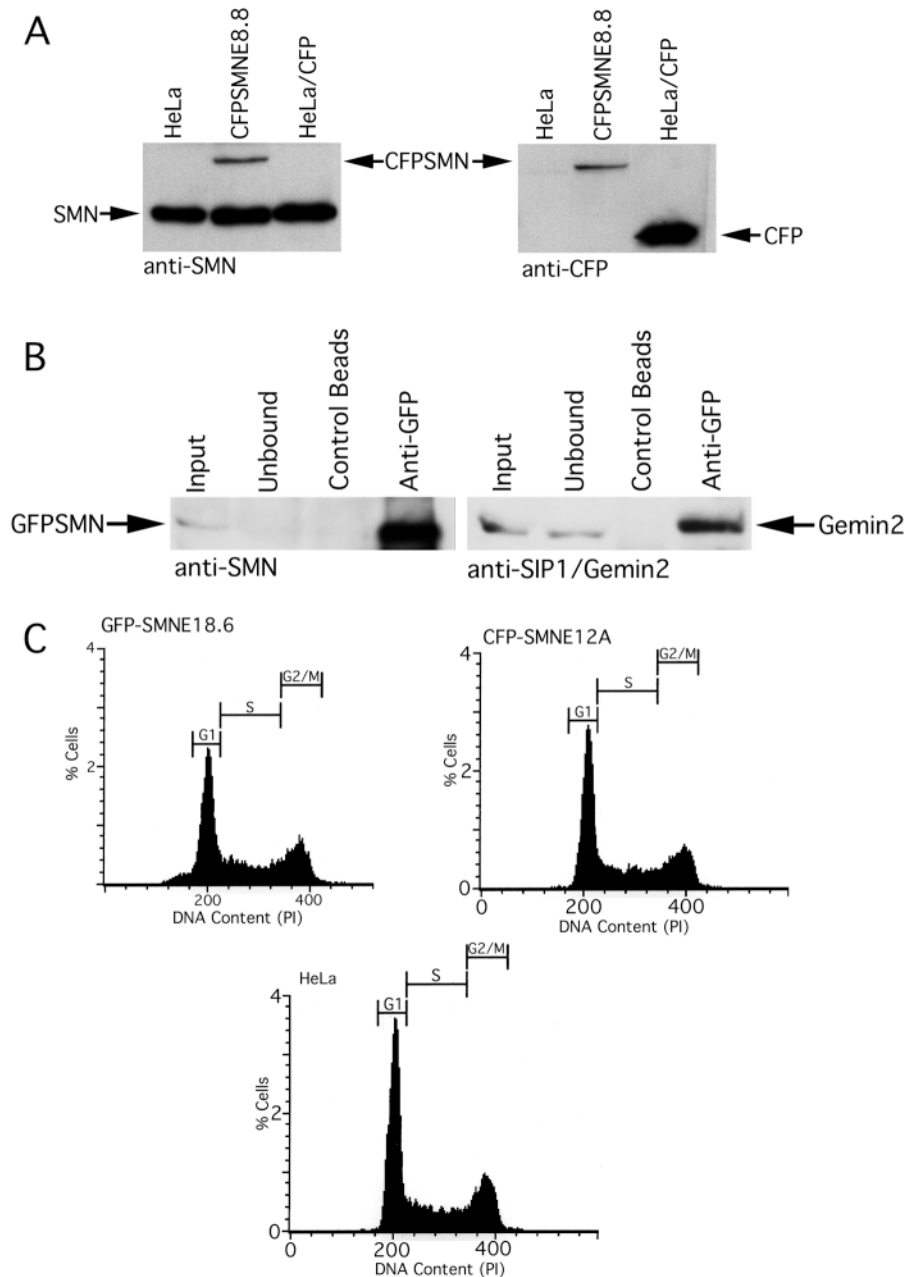


Fig. 2. FP-SMN is expressed at low levels relative to endogenous SMN, interacts with SIP1/Gemin2 and does not affect cell cycle. (A) Total cell lysates from the parental HeLa cell line, line CFP-SMNE8.8 and parental HeLa cells transiently transfected with a plasmid expressing CFP probed with anti-SMN and anti-FP antibodies. All three cell lines give a strong band at 38 kDa with anti-SMN, representing endogenous SMN. Line CFP-SMNE8.8 shows an additional, much weaker, band at 68 kDa, representing stably expressed CFP-SMN. A band of the same size is detected in line CFP-SMNE8.8 using the anti-FP antibody, whereas parental HeLa cells transiently transfected with CFP alone give a single band at 30 kDa. (B) Co-immunoprecipitations from total cell lysates of line GFP-SMNE10.3 using anti-FP antibodies. Detection of products using anti-SMN antibodies demonstrates the presence of GFP-SMN in the input material and the immunoprecipitated material (anti-GFP lane). A duplicate blot probed with anti-SIP1/Gemin2 shows a clear enrichment of SIP1/Gemin2 in the immunoprecipitated fraction (anti-GFP lane). (C) FACS analysis of synchronised cell populations stained with propidium iodide shows a similar profile for lines GFP-SMNE18.6, CFP-SMNE12A and the parental HeLa cell line.

endogenous SMN (Fig. 2A, left-hand panel). Probing with anti-FP antibodies shows a single band in the lysate from cell line CFP-SMNE8.8 representing CFP-SMN (Fig. 2A, right-hand panel), confirming that the CFP signal seen in the cell line is full-length CFP-SMN. No free CFP or truncated CFP fusion proteins are detected.

We next tested whether the stably expressed FP-fusion proteins can be immunoprecipitated with anti-FP antibodies and whether they interact with the core SMN-complex protein SIP1/Gemin2. Both GFP-SMN (Fig. 2B) and CFP-SMN (data not shown) can be efficiently immunoprecipitated using antibodies to GFP. The left-hand panel, detected with anti-SMN, shows total lysate from cell line GFP-SMNE18.6 (input) and the material immunoprecipitated using anti-FP antibodies. The right-hand panel shows duplicate samples detected using anti-SIP1/Gemin2 antibodies. This confirms that a large

proportion of the SIP1/Gemin2 from this cell line is co-immunoprecipitated with GFP-SMN. Thus, FP-SMN is in a complex with endogenous SIP1/Gemin2, a core member of the SMN complex, in the stable cell lines.

We next analysed the growth properties of the stable cell lines to see whether expression of FP-SMN affects cell cycle progression. The growth rate of each FP-SMN cell line is similar to that of the parental HeLa cell line (data not shown). Furthermore, FACS analysis (Fig. 2C) demonstrates that, in both stable cell lines, a similar proportion of cells are in G1, S and G2 stages of the cell cycle as in the parental HeLa cell line.

We conclude that constitutive low-level expression of FP-SMN in stable HeLa cell lines does not prevent cell cycle progression or alter their growth rate. Furthermore, the FP-tagged proteins maintain *in vivo* interactions shown by the endogenous SMN protein.

Over-expression of FP-SMN induces cytoplasmic structures containing SMN complex and core snRNP proteins

We observed that, both following transient transfection of cells with plasmid vectors encoding FP-SMN, and during early stages of the establishment of the stable cell lines, some

cells expressed high levels of FP-SMN as judged by fluorescence microscopy. These cells did not survive the selection process and no cell lines expressing high levels of FP-SMN were obtained, suggesting that over-expression of SMN may be toxic. Closer examination of HeLa and MCF-7 cells over-expressing SMN showed that they had large accumulations of FP-SMN in the cytoplasm, coupled with either an absence of nuclear CBs (Fig. 3B,E) or a large number of very small nuclear CBs (Fig. 3H,K,N). The cytoplasmic FP-SMN accumulations also contained the SMN complex protein SIP1/Gemin2 (Fig. 3A-F, arrows), and the core snRNP, Sm proteins (Fig. 3G-I). They did not contain either TMG-capped snRNA (Fig. 3J-L, arrows) or the CB protein, coilin (Fig. 3M-O). The small nuclear bodies seen contain Sm proteins (Fig. 3G-I), TMG-capped snRNA (Fig. 3J-L, arrows) and coilin (Fig. 3M-O, arrows). Thus, whereas constitutive low expression of FP-SMN has no obvious deleterious effects on cells, transient over-expression appears toxic and results in the accumulation of both the SMN-complex and Sm proteins in the cytoplasm, and an additional disruption of nuclear bodies.

To confirm that this effect was caused by increased levels of FP-SMN, cells from line GFP-SMNE18.6 were transiently transfected with plasmid pECFP-SMN expressing CFP-SMN (Fig. 4). This resulted in cytoplasmic accumulations of both GFP-SMN (A) and CFP-SMN (B) specifically in the transfected cells.

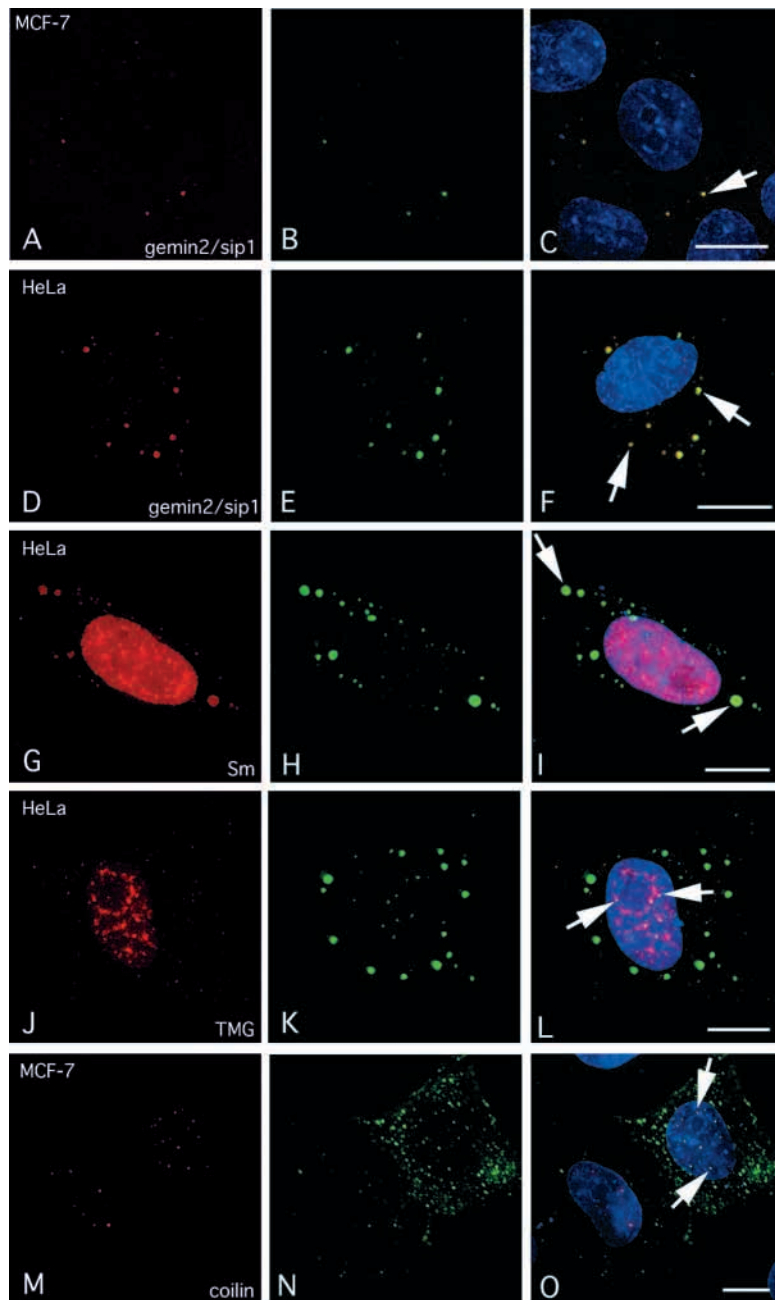


Fig. 3. High-level expression of FP-SMN leads to cytoplasmic accumulation of SMN-complex proteins and disruption of nuclear structure. Three-dimensional projections of serial sections showing HeLa cells and MCF-7 cells expressing high levels of GFP-SMN following transient transfection. All cells show cytoplasmic accumulation of GFP-SMN (arrows in C, F and I). These accumulations also contain SIP1/Gemin2 (A-F) and Sm proteins (G-I). They do not contain TMG-capped RNA (J-L) or coilin (M-O). Many cells also show a large number of small nuclear bodies containing GFP-SMN, TMG-capped RNA and coilin (arrows in L and O). Bar, 10 μ m.

CBs labelled with either FP-SMN or FP-coilin show similar dynamics during interphase

Time-lapse analyses were performed to examine the dynamic behaviour of CBs containing SMN in interphase cells (see Materials and Methods). Analysis of the movements of Cajal bodies demonstrates that CBs are dynamic structures in cell line GFP-SMNE18.6. In addition to constant small movements, CBs were seen to join together (Fig. 5A), separate to form two bodies (Fig. 5B) and move in close proximity to each other without joining (Fig. 5C). This mirrors the dynamic behaviour previously reported using a stable HeLa expressing GFP-coilin under a tetracycline-inducible promoter (Platani et al., 2000). Similar dynamic behaviour was also seen for CBs in a stable cell line derived from the same parental HeLa cell line expressing YFP-coilin under a constitutive promoter (cell line EYFP-CoilinE1.1.1) (J.E.S. and A.I.L., unpublished). The frequency of each type of movement is shown in Fig. 5D. Using GFP-SMN as a marker, small CBs are also occasionally observed to appear or disappear within the nucleoplasm. These data demonstrate that the dynamic properties of CBs are not dependent upon, or apparently affected by, the presence of different labelled marker proteins.

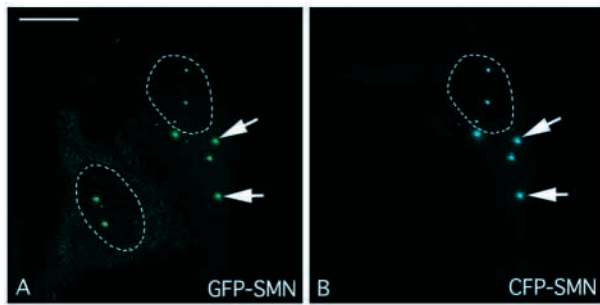


Fig. 4. Cytoplasmic accumulations of FP-SMN can be induced by expressing CFP-SMN in a GFP-SMN stable cell line. Three-dimensional projections of deconvolved serial sections of cells from line GFP-SMNE10.3 transiently transfected with a plasmid encoding CFP-SMN. An untransfected cell (A, bottom left) shows the characteristic SMN distribution of diffuse cytoplasmic signal and nuclear Cajal bodies. A transiently transfected cell (A top right, and B) shows accumulation of GFP-SMN and CFP-SMN in the cytoplasm (arrows). Note: with this combination of FP proteins, a small amount of bleed-through is seen from CFP-SMN into the GFP image, but no bleed-through is observed from GFP-SMN into the CFP channel. Bar, 10 μ m.

Differential dynamics of GFP-SMN and YFP-coilin within Cajal bodies

To compare the dynamics of SMN and coilin proteins within CBs, FRAP experiments were performed on cells from line GFP-SMNE10.3 and from line YFP-coilinE1.1.1. Fluorescence signal was bleached from individual CBs (Fig. 6A,B), using conditions that bleached the signal from the entire structure, and single confocal sections recorded at either 4- or 5-second intervals during recovery. The YFP-coilin signal returned rapidly to CBs, with a plateau of 50% recovery reached by 40 seconds. Half of this recovery was attained within the first 10 seconds (Fig. 6A). Similar results were obtained in cells transiently transfected with GFP-coilin (data not shown). In contrast, GFP-SMN showed no appreciable return to Cajal bodies over a 1 minute recovery period (Fig. 6B). To investigate further the dynamics of SMN in CBs, a longer time course was performed, collecting a series of confocal sections through the cell over a 1 hour recovery period (Fig. 6C). In this time, GFP-SMN did show an appreciable return to CBs, regaining almost half of the original signal within 1 hour (Fig. 6C). Interestingly, although no appreciable loss of signal from CBs because of the imaging was seen in a

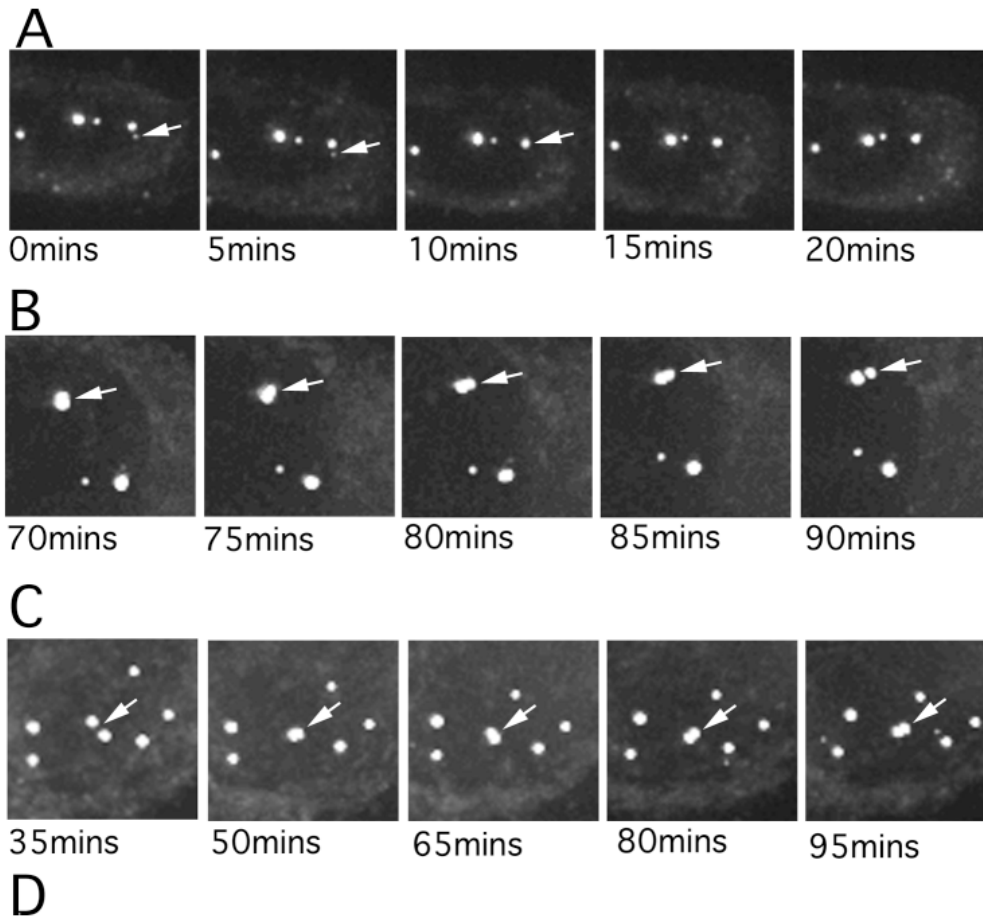


Fig. 5. Time-lapse analysis of interphase cells shows fusion and separation of GFP-SMN Cajal bodies and close interactions between bodies. A-C show 3D projections of serial sections of living cells from line GFP-SMNE10.3 taken from a time series. (A) Fusion of a small body (arrow) with a larger one. (B) Separation of a large body (arrow) into two smaller ones. (C) Close interaction between two bodies (arrow). The frequency of these and other events are shown in panel D.

No. of nuclei	No. of Cajal bodies	Joining events	Separations	Close interactions	Appearances	Disappearances
43	208	4	2	11	2	1

Time courses taken on 5 separate occasions, between 2hrs 5 mins and 2.5 hrs duration.

neighbouring cell, a significant loss of signal was seen from unbleached CBs in the nucleus containing the bleached CB. This apparent FLIP effect suggests that at least some of the recovered GFP-SMN was recruited from neighbouring CBs. In parallel FLIP experiments, a region of the cytoplasm was repeatedly bleached and the resulting effect on the fluorescence of GFP-SMN in CBs monitored using serial confocal sections

collected after each bleaching event (Fig. 6D). Each bleaching event took 5 seconds, with an imaging time of approximately 10 seconds at each time point. Fluorescence signal was rapidly lost from CBs in bleached cells, with half of the signal lost after 2 to 4 bleaching events.

There appears to be a rapid exchange of SMN from CBs into the cytoplasm, because bleaching of the cytoplasmic GFP-SMN

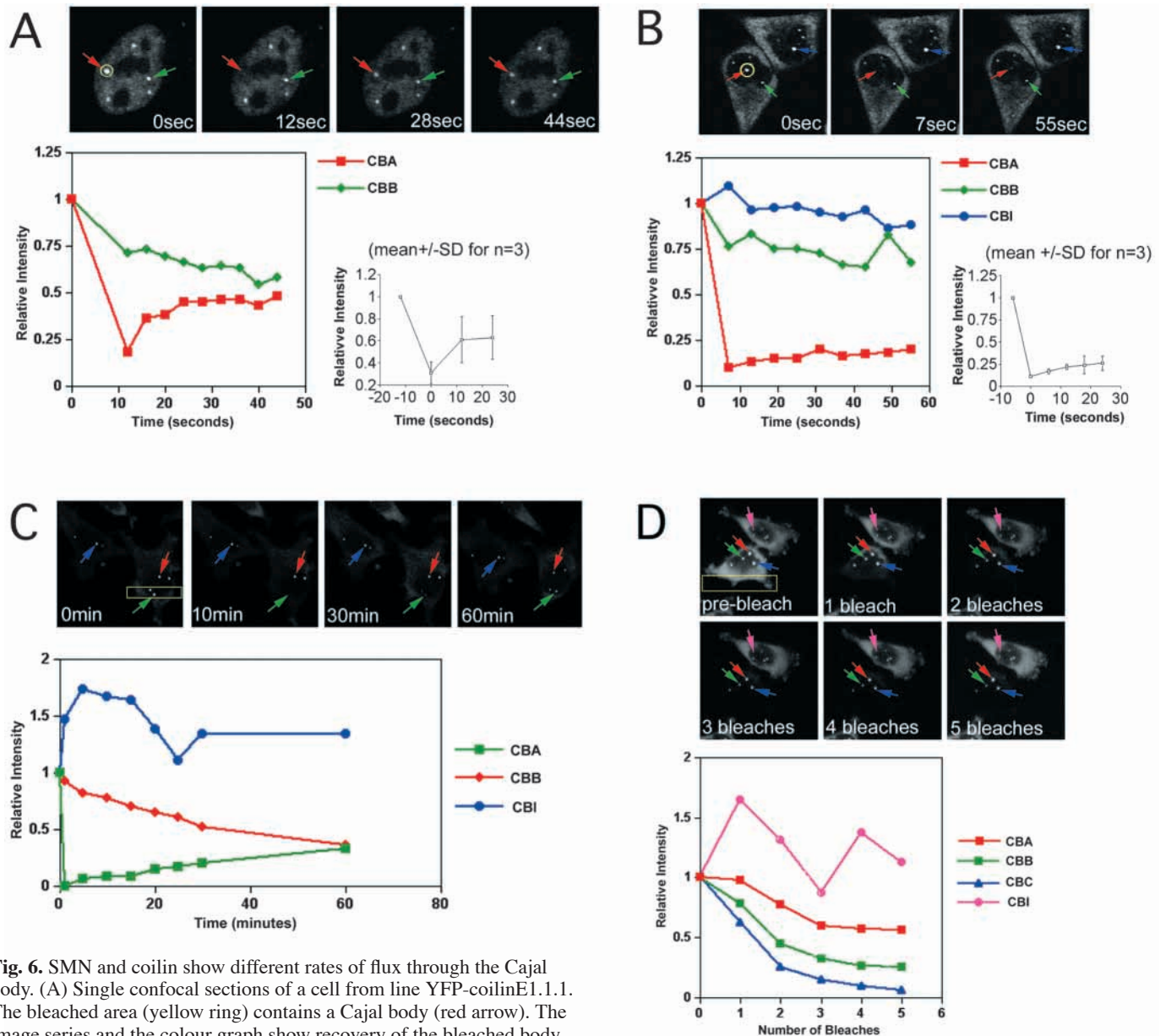


Fig. 6. SMN and coilin show different rates of flux through the Cajal body. (A) Single confocal sections of a cell from line YFP-coilinE1.1.1. The bleached area (yellow ring) contains a Cajal body (red arrow). The image series and the colour graph show recovery of the bleached body compared to the intensity of an unbleached body (green arrow) in the same nucleus. The greyscale graph shows averaged data from bleached CBs in three separate cells. (B) Single confocal sections of a cell from line GFP-SMNE10.3. The bleached area (yellow ring) contains a Cajal body (red arrow). The image series and the graph show recovery of the bleached body compared to the intensity of an unbleached body (green arrow) in the same nucleus and an unbleached body (blue arrow) in a neighbouring nucleus. The greyscale graph shows averaged data from bleached CBs in three separate cells. (C) Three-dimensional projection of series of confocal sections through a cell from line GFP-SMNE10.3. The bleached area (yellow box) contains a Cajal body (green arrow). The image series and the graph show recovery of the bleached body compared to the intensity of an unbleached body (blue arrow) in a neighbouring nucleus. (D) Three-dimensional projection of series of confocal sections through a cell from line GFP-SMNE10.3. The bleached area (yellow box) encompasses a large region of cytoplasm. The image series and graph show the progressive loss of signal from Cajal bodies in the bleached cell over successive bleaches (green, red and blue arrows) compared to a Cajal body in a neighbouring cell (pink arrow).

signal results in rapid loss of GFP-SMN from CBs. Considering that it takes ~1 hour for recovery of ~50% GFP-SMN signal in CBs following direct photobleaching of CBs, the rapid loss of GFP-SMN signal from CBs after bleaching the cytoplasm is unlikely to be a result of a rapid incorporation into CBs of bleached GFP-SMN molecules from the cytoplasm. Instead, the data suggest that the nuclear pool of SMN undergoes relatively rapid transport back to the cytoplasm.

Dynamics of Cajal body markers through mitosis

It is known that both snRNPs and p80 coilin are present in bodies during mitosis. However, there are at least two classes of snRNP-containing bodies in mitotic cells, some of which co-localise with p80-coilin and some of which do not (Ferreira et al., 1994). In addition, the co-localisation of coilin with SMN has been seen to persist through mitosis, although coilin re-enters the nucleus earlier than SMN, which is targeted to pre-formed Cajal bodies (Carvalho et al., 1999). The ability to follow live cells expressing GFP-SMN during mitosis allows a direct analysis of the dynamics of these mitotic CB remnants. The top three rows of Fig. 7 show three separate cells from line GFP-SMNE10.3 undergoing mitosis. During prophase,

metaphase, anaphase and telophase, a small number of GFP-SMN-positive bodies are seen (Ai to v and Bi). During late telophase, however, a large number of GFP-SMN bodies form rapidly (Bii to v, Ci and ii). As the daughter cells begin to flatten out, these bodies rapidly disappear, prior to the appearance of the normal interphase distribution of GFP-SMN in a diffuse cytoplasmic pool with a small number of nuclear bodies (Ciii to v). Cells expressing YFP-coilin were also followed through mitosis (Fig. 7D,E). In marked contrast to the behaviour of GFP-SMN, YFP-coilin is seen in a small number of bodies only as far as anaphase (Di and ii). During telophase, YFP-coilin is rapidly imported into the forming daughter nuclei (Diii to v). As the daughter cells flatten out, nuclear bodies can be seen to form either distant from (arrow) or close to (arrowhead) nascent nucleoli. Because it is recognised that SMN is targeted to pre-formed nuclear CBs that already contain coilin (Carvalho et al., 1999), the initial appearance of coilin-positive bodies can be concluded to be the initial formation of nuclear CBs in the daughter nuclei. It is, therefore, interesting to note that they can form in close proximity to a nucleolus, but do not always form at the nucleolar periphery, supporting the view that there may be several different mechanisms for CB formation.

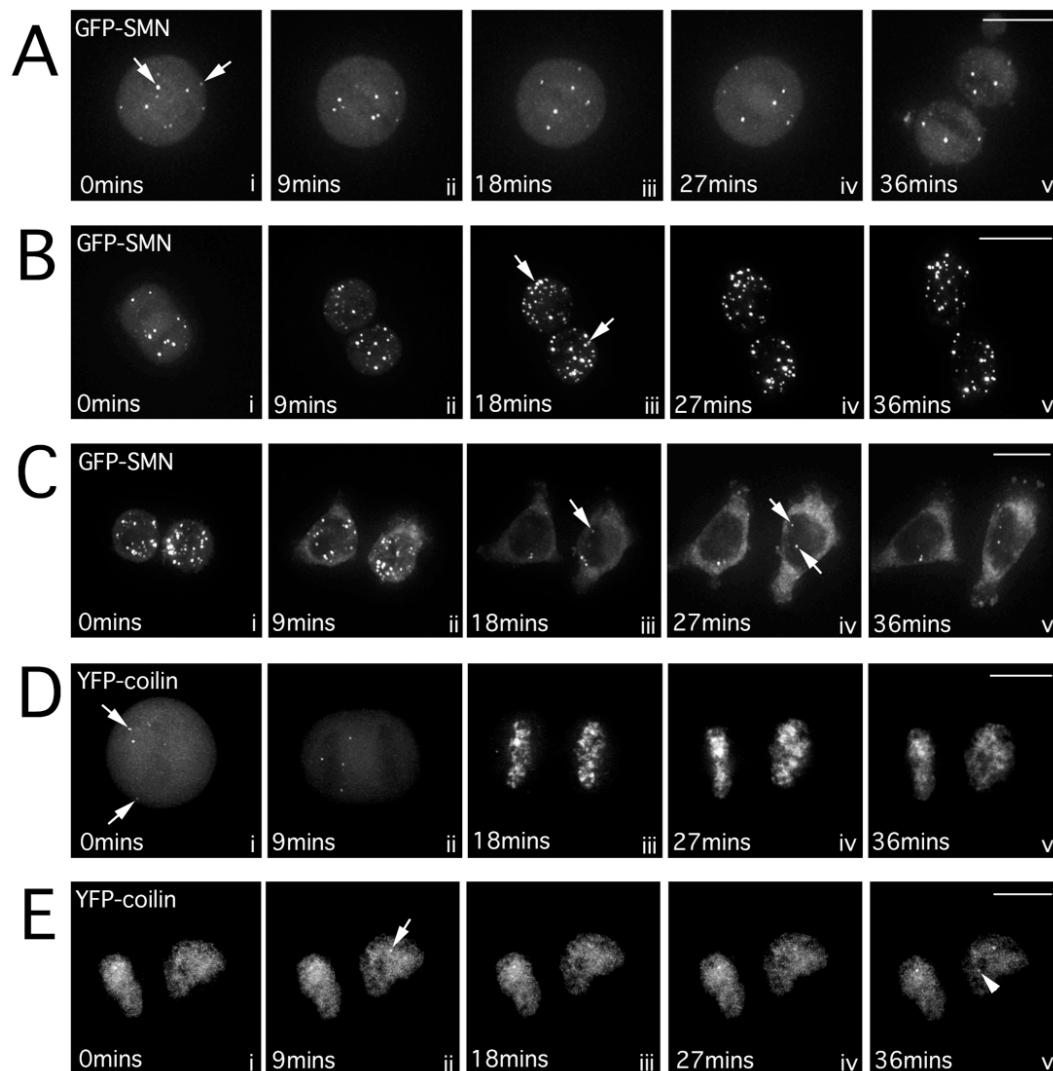


Fig. 7. Dynamics of GFP-SMN and YFP-coilin through mitosis. (A) Three-dimensional projections of serial sections from a time series of line GFP-SMNE10.3 from prophase through to telophase. Mitotic Cajal bodies (MCBs) are arrowed. (B) GFP-SMNE10.3 through telophase. Large numbers of small SMN-positive bodies (arrows) appear in late telophase. (C) GFP-SMNE10.3 from telophase to G1. The SMN-positive bodies disappear as GFP-SMN begins to accumulate in nuclear Cajal bodies (arrows). (D) Three-dimensional projections of serial sections from a time series of line YFP-coilinE1.1.1 from prophase through to telophase. Mitotic Cajal bodies are arrowed. (E) YFP-coilinE1.1.1 in G1. Coilin-positive Cajal bodies are seen to form either distant from (arrow) or near to (arrowhead) nascent nucleoli.

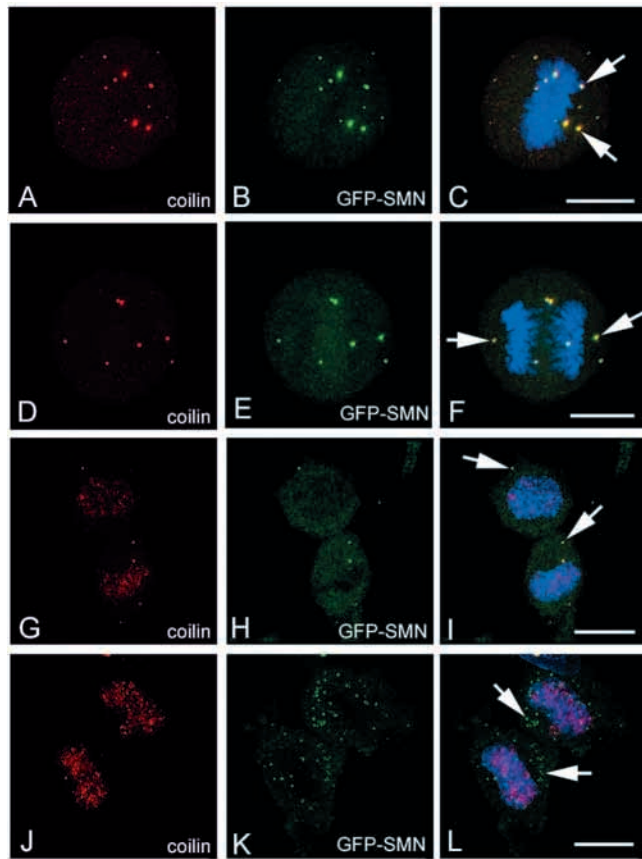


Fig. 8. SMN and coilin co-localise in mitotic Cajal bodies (MCBs) until telophase. Three-dimensional projections of deconvolved serial sections through cells of line GFP-SMNE10.3 in metaphase (A-C), anaphase (D-F), telophase (G-I) and cytokinesis (J-L) counterstained with anti-coilin antibodies (red). GFP-SMN and coilin co-localise until late telophase (arrows in C, F and I). This association is lost soon after the re-import of coilin into the forming nuclei as the daughter cells flatten out, leaving a large number of SMN-positive bodies in the cytoplasm (arrows in L). Bar, 10 μ m.

Mitotic bodies containing SMN differ in their composition from those caused by GFP-SMN over-expression in interphase cells

Immunostaining of cells from line GFP-SMNE10.3 with antibodies to coilin demonstrates that both SMN and coilin are present in the same bodies during mitosis until late telophase (Fig. 8A-F). The association persists as coilin begins to enter the newly formed nuclei (Fig. 8G-I) but is subsequently lost as coilin continues to concentrate in the nuclei and GFP-SMN begins to form the numerous, smaller cytoplasmic bodies seen in the time-lapse studies. Further analysis of the composition of the mitotic CB remnants demonstrates that they contain both Sm proteins (Fig. 9A-H) and TMG-capped RNA (Fig. 9I-L). The presence of TMG-capped RNA and coilin sets these structures apart from the cytoplasmic accumulations of SMN-complex proteins that result from the over-expression of GFP-SMN in interphase cells (Fig. 3). It is also interesting to note that bodies are present in mitosis that contain TMG-capped RNA in the absence of SMN or coilin (Fig. 9I arrowheads). These may represent snRNAs that had been transcribed but not yet begun assembly into snRNPs prior to the onset of mitosis.

Discussion

Here we report a comparison of the dynamics of fluorescently tagged Cajal body proteins GFP-SMN and YFP-coilin. Although SMN and coilin show similar sub-nuclear localisations, they show very different dynamics of exchange into and out of CBs. Furthermore, these two proteins show dramatically different dynamics of re-import into the nucleus following mitosis. The behaviour of CB components during mitosis is reminiscent of that of nucleolar components (Dundr et al., 2000), demonstrating further similarities between these two nuclear structures.

At the cellular level, the reduction in expression of the SMN protein in SMA is associated with a failure of the SMN complex to assemble into nuclear bodies (Covert et al., 1997; Lefebvre et al., 1997; Frugier et al., 2000). The restriction of the disease

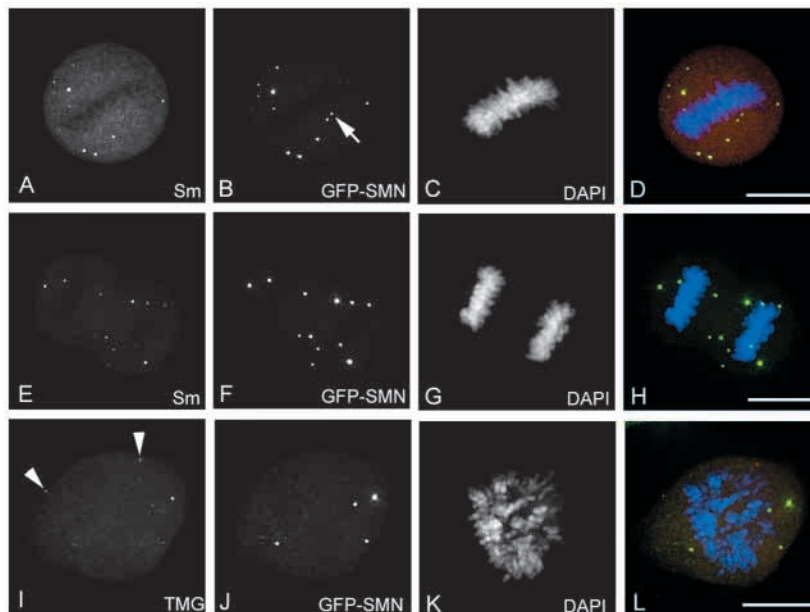


Fig. 9. Mitotic Cajal bodies (MCBs) contain Sm proteins and TMG-capped RNA. Three-dimensional projections of deconvolved serial sections through cells of line GFP-SMNE10.3 in mitosis counterstained with antibodies to Sm proteins (A-H) and TMG-capped RNA (I-L). The majority of SMN-positive bodies also contain Sm proteins and TMG-capped RNA, although some bodies contain SMN in the absence of Sm proteins (arrows in B) and some contain TMG-capped RNA in the absence of SMN (arrowheads in I). The overlays (D, H and L) show GFP-SMN in green and antibody staining in red. Bar, 10 μ m.

phenotype to motor neurons, despite a systemic decrease in SMN expression, has led to the suggestion that most human cells express SMN in excess of their needs, whereas motor neurons express only the amount they require. This would make motor neurons uniquely sensitive to depletion of the protein (Wang and Dreyfuss, 2001). Observation of cells expressing high levels of FP-SMN in this study, however, suggest a more complex regulation of SMN and its associated proteins. Over-expression of FP-SMN in HeLa or MCF-7 cells leads to the appearance of cytoplasmic accumulations of FP-SMN (Figs 3, 4), which also contain the SMN-complex protein SIP1/Gemin2 and Sm proteins. Importantly, TMG-capped RNA is absent from these accumulations, suggesting that they may represent SMN complexes blocked at an early stage of snRNP assembly, similar to the cytoplasmic block previously shown to be induced by expression of a myc-tagged deletion mutant of SMN (SMN Δ 27) (Pellizzoni et al., 1998). Furthermore, over-expression of SMN leads to a disruption of CBs within the nucleus, where we observed a proliferation of small bodies containing SMN, coilin, Sm proteins and TMG-capped snRNAs. This suggests that, although coilin is required for the recruitment of SMN and Sm proteins to CBs (Tucker et al., 2001; Hebert et al., 2001), the level of SMN expression may have a role in determining the size and number of CBs formed.

FP-SMN provides a specific marker for CBs that accumulate newly imported snRNPs

CB dynamics have been studied using GFP-U2B'' in plant cells (Boudonck et al., 1999) and GFP-SmD1 (Sleeman et al., 1998), GFP-fibrillarin (Snaar et al., 2000) and GFP-coilin in mammalian cells (Platani et al., 2002; Platani et al., 2000). Time-lapse analysis of FP-SMN cell lines in interphase reveals similar types of movements and interactions between CBs as seen previously using other GFP-tagged proteins as markers to label CBs (Fig. 5). Fusions between bodies (A), separations of bodies into two (B) and close interaction between bodies (C) were all seen with a similar frequency as in cells from the same parental HeLa line expressing YFP-coilin. In addition to establishing FP-SMN as a useful marker for following the movement of CBs in living cells, this also suggests that low level over-expression of either FP-SMN or FP-coilin does not, in itself, alter CB dynamics. The CBs involved in the accumulation of new snRNPs on re-entry into the nucleus are specifically those that contain SMN-complex proteins (Carvalho et al., 1999; Sleeman and Lamond, 1999a). Indeed, the transient expression of tagged core snRNP, Sm, proteins leads to the formation of CBs in primary cells that do not normally contain them (Sleeman et al., 2001). In light of the existence, in some cell types, of coilin-positive CBs that lack SMN, we can now be certain, using the FP-SMN cell lines, that the CBs studied are specifically those containing SMN-complex proteins implicated in snRNP maturation.

GFP-SMN and YFP-coilin show markedly different dynamics of interaction with CBs

Despite the similarities in the dynamic behaviour of CBs seen using either FP-SMN or FP-coilin as markers, FRAP experiments demonstrate that the flux of these two proteins through CBs are different. Thus, whereas YFP-coilin reaches

a plateau of recovery of signal to a bleached CB within one minute, with most of this recovery seen in the first 10 seconds, GFP-SMN shows minimal recovery over this time period, with 1 hour required to recover 50% of the original GFP-SMN fluorescence. At first sight, this may seem intuitive as, judged by immunofluorescence microscopy, there appears to be a more substantial nucleoplasmic pool of coilin than of SMN. However, previous studies using GFP-fibrillarin, which also has a small nucleoplasmic pool, showed a rapid recovery of the tagged protein following bleaching of either a nucleolus (Phair and Misteli, 2000) or CBs (Snaar et al., 2000). Furthermore, the recovery of YFP-coilin to CBs was also rapid in cells in which the nucleoplasmic pool of YFP-coilin was perceived by microscopy to be extremely low (data not shown). The rate of recovery of YFP-coilin to CBs was similar to that previously reported for the recovery of the splicing factor, ASF/SF2 to speckles (Phair and Misteli, 2000; Kruhlak et al., 2000). It has been demonstrated that coilin has the ability to self-associate (Hebert and Matera, 2000). The presence of the coilin self-interacting domain is both necessary and sufficient for the localisation of coilin to CBs. In contrast, SMN, although also capable of self-interaction (Lorson et al., 1998), requires the presence of coilin for its recruitment into CBs (Tucker et al., 2001; Hebert et al., 2001). SMN and SmB have been demonstrated to compete for binding to coilin, leading to the suggestion that coilin may also have a role in the dissociation of the SMN-snRNP complex (Hebert et al., 2001). Our current observations show a rapid turnover of coilin in CBs and a much slower turnover of SMN. This is consistent with the idea of a simple molecular interaction between coilin molecules leading to the incorporation of coilin into the CB, with a more complex, multi-molecular interaction being required for the association and disassociation of SMN from the CB.

FLIP experiments demonstrate that repeated bleaching of the cytoplasmic pool of GFP-SMN leads to a rapid loss of GFP-SMN from nuclear CBs. Taken together with the slow recovery of GFP-SMN into nuclear CBs, with concomitant loss of signal from neighbouring CBs, this suggests that the GFP-SMN in CBs is able to return to the cytoplasm, so that depletion of the cytoplasmic pool also directly depletes the nuclear pool of SMN. Although it is increasingly probable that SMN accompanies newly formed snRNPs from the cytoplasm into the nucleus via CBs (Carvalho et al., 1999; Sleeman et al., 2001; Narayanan et al., 2002), less is known about any return transport of SMN to the cytoplasm.

Dynamics of Cajal body markers through mitosis

In addition to differences in the flux of coilin and SMN through CBs, the dynamic behaviour of the two proteins during their re-entry into the nucleus following mitosis is also different. From prophase through to telophase, coilin and SMN co-localise in a small number of mitotic CB remnants (MCBs). These structures differ from the cytoplasmic SMN accumulations resulting from over-expression of FP-SMN in that they contain both coilin and, in most cases, TMG-capped RNA, in addition to SMN and Sm proteins. Rather than representing SMN-snRNP complexes blocked in their assembly, as the interphase cytoplasmic accumulations most probably do, we suggest that these structures may represent a way to preserve essential SMN-snRNP processing complexes

during mitosis. A similar phenomenon has been reported for rRNA processing complexes during mitosis (Dundr et al., 2000). In this case, partially processed rRNA is seen to co-localise with several of its processing components (fibrillarin, nucleolin and B23) through mitosis in nucleolus-derived foci (NDFs). In contrast to NDFs, MCBs do not contain detectable levels of fibrillarin, nucleolin or B23 (J.E.S. and A.I.L., unpublished), so appear to be separate structures. It is probable, therefore, that the partial preservation of RNA processing complexes during mitosis is a feature common to snRNAs and rRNAs and, importantly, common to CBs and nucleoli, whose roles in these processing events may be related and linked to each other. Nucleoli and CBs contain many common factors, such as fibrillarin, Nopp140 and snoRNAs, suggesting that the two structures have co-operative roles in ribosome production, with the CB involved in the maturation of macromolecular complexes, such as snoRNPs, essential for rRNA processing in the nucleolus (reviewed by Terns and Terns, 2001; Gall, 2000). Events required for the maturation of snoRNPs may well be similar to those required for the maturation of splicing snRNPs, in which the CB probably participates. Furthermore, under certain conditions, coilin and snRNP proteins are found inside nucleoli (Ochs et al., 1994; Malatesta et al., 1994; Lyon et al., 1997; Sleeman et al., 1998). It is probable that the nucleolus has roles in processes other than rRNA processing (reviewed by Pederson, 1998). The morphological link between nucleoli and CBs has been evident from their initial description as nucleolar accessory bodies (Ramon-y-Cajal, 1903). The similarities in their molecular composition and potential joint roles in the processing of many RNA species are becoming increasingly apparent (reviewed by Gall, 2000).

Mitotic CBs containing coilin and snRNP proteins have been reported previously (Ferreira et al., 1994) and the co-localisation of SMN and coilin in these structures has been described (Carvalho et al., 1999). Here we present the first dynamic analysis of MCBs, which reveals striking differences in the re-entry of coilin and SMN into the forming daughter nuclei. The MCBs are extremely mobile within the cell, making tracking of individual bodies problematic using a frequency of imaging that can be tolerated by mitotic cells (Fig. 7A,D). This is in marked contrast to the behaviour of nuclear CBs during interphase, in which the basic spatial arrangement of CBs is often more stable (Fig. 5) and may be because of the huge rearrangements of cellular structure that occur during mitosis. These data are, therefore, suggestive of a role for rearrangements of areas of the nucleus, perhaps including the re-organisation of chromatin, for large movements of interphase CBs.

At the end of telophase, GFP-SMN rapidly forms a large number of punctate cytoplasmic structures of various sizes. This event is usually concomitant with a perceived decrease in the amount of diffuse GFP-SMN. These highly mobile structures persist for approximately 20 minutes, then rapidly disappear, immediately prior to the re-appearance of GFP-SMN in nuclear CBs. In contrast, YFP-coilin is rapidly lost from MCBs early in telophase, when the protein is imported into the forming daughter nuclei. Initially showing a 'clumped' distribution, the YFP-coilin gradually becomes more diffuse as the nuclei flatten out. In early G1, CBs re-form within the daughter nuclei. Because coilin is observed in CBs before SMN (Carvalho et al., 1999) (J.E.S. and A.I.L., unpublished),

this most probably represents the initial formation of nuclear CBs. It is interesting, therefore, to note that CB formation is seen both in proximity to (Fig. 7E, arrowhead) and distant from (Fig. 7E, arrow) nascent nucleoli. Electron microscopy studies of CBs in close proximity to nucleoli have shown CBs to have a close structural relationship to nucleoli, appearing either to fuse with or bud from nucleoli. Although not ruling out the possibility that CBs can form at the nucleolar periphery, our current data indicate that CBs can form within the nucleoplasm at some distance from nucleoli.

In summary, we have established stable HeLa cell lines expressing SMN fused to fluorescent proteins and compared them with cells stably expressing FP-tagged coilin. The two CB proteins, SMN and coilin, although showing similar distributions within the nucleus, show very different rates of flux through nuclear CBs, presumably related to differences in the complexity of the interactions that cause their accumulation in CBs. The dynamic behaviour of the two proteins through mitosis and during the reformation of nuclear structures following mitosis show further differences between SMN and coilin, but reveal parallels in the behaviour of the nucleolar rRNA processing machinery and the snRNA processing machinery normally resident in CBs.

We thank G. Morris for antibodies MANSMA1 and MANSIP1; B. Frenguelli and C. Connolly for use of the LSM510. This work was supported by the Wellcome Trust. A.I.L. is a Wellcome Trust Principal Research Fellow.

References

- Andrade, L. E., Chan, E. K., Raska, I., Peebles, C. L., Roos, G. and Tan, E. M. (1991). Human autoantibody to a novel protein of the nuclear coiled body: immunological characterization and cDNA cloning of p80-coilin. *J. Exp. Med.* **173**, 1407-1419.
- Bachand, F., Boisvert, F., Cote, J., Richard, S. and Autexier, C. (2002). The product of the survival of motor neuron (SMN) gene is a human telomerase-associated protein. *Mol. Biol. Cell* **13**, 3192-3202.
- Bohmann, K., Ferreira, J. A. and Lamond, A. I. (1995). Mutational analysis of P80 Coilin indicates a functional interaction between coiled bodies and the nucleolus. *J. Cell Biol.* **131**, 817-831.
- Boudonck, K., Dolan, L. and Shaw, P. J. (1999). The movement of coiled bodies visualized in living plant cells by the green fluorescent protein. *Mol. Biol. Cell* **10**, 2297-2307.
- Carvalho, T., Almeida, F., Calapez, A., Lafarga, M., Berciano, M. T. and Carmo-Fonseca, M. (1999). The spinal muscular atrophy disease gene product, SMN: a link between snRNP biogenesis and the Cajal (coiled) body. *J. Cell Biol.* **147**, 715-728.
- Covert, D. D., Le, T. T., McAndrew, P. E., Strasswimmer, J., Crawford, T. O., Mendell, J. R., Coulson, S. E., Androphy, E. J., Prior, T. W. and Burghes, A. H. (1997). The survival motor neuron protein in spinal muscular atrophy. *Hum. Mol. Genet.* **6**, 1205-1214.
- Darzacq, X., Jady, B. E., Verheggen, C., Kiss, A. M., Bertrand, E. and Kiss, T. (2002). Cajal body-specific small nuclear RNAs: a novel class of 2'-O-methylation and pseudouridylation guide RNAs. *EMBO J.* **21**, 2746-2756.
- Dundr, M., Misteli, T. and Olson, M. O. (2000). The dynamics of postmitotic reassembly of the nucleolus. *J. Cell Biol.* **150**, 433-446.
- Ferreira, J. A., Carmofonseca, M. and Lamond, A. I. (1994). Differential interaction of splicing snRNPs with coiled bodies and interchromatin granules during mitosis and assembly of daughter cell nuclei. *J. Cell Biol.* **126**, 11-23.
- Fischer, U., Liu, Q. and Dreyfuss, G. (1997). The SMN-SIP1 complex has an essential role in spliceosomal snRNP biogenesis. *Cell* **90**, 1023-1029.
- Fischer, U., Sumpter, V., Sekine, M., Satoh, T. and Luhrmann, R. (1993). Nucleo-cytoplasmic transport of U snRNPs: definition of a nuclear location signal in the Sm core domain that binds a transport receptor independently of the m3G cap. *EMBO J.* **12**, 573-583.

- Frugier, T., Tiziano, F. D., Cifuentes-Diaz, C., Miniou, P., Roblot, N., Dierich, A., Le-Meur, M. and Melki, J. (2000). Nuclear targeting defect of SMN lacking the C-terminus in a mouse model of spinal muscular atrophy. *Hum. Mol. Genet.* **9**, 849-858.
- Gall, J. G. (2000). Cajal bodies: the first 100 years. *Annu. Rev. Cell Dev. Biol.* **16**, 273-300.
- Hamm, J., Darzynkiewicz, E., Tahara, S. M. and Mattaj, I. W. (1990). The trimethylguanosine cap structure of U1 snRNA is a component of a bipartite nuclear targeting signal. *Cell* **62**, 569-577.
- Hebert, M. D. and Matera, A. G. (2000). Self-association of coilin reveals a common theme in nuclear body localization. *Mol. Biol. Cell* **11**, 4159-4171.
- Hebert, M. D., Szymczyk, P. W., Shpargel, K. B. and Matera, A. G. (2001). Coilin forms the bridge between Cajal bodies and SMN, the spinal muscular atrophy protein. *Genes Dev.* **15**, 2720-2729.
- Jablonka, S., Holtmann, B., Meister, G., Bandilla, M., Rossoll, W., Fischer, U. and Sendtner, M. (2002). Gene targeting of Gemin2 in mice reveals a correlation between defects in the biogenesis of snRNPs and motoneuron cell death. *Proc. Natl. Acad. Sci. USA* **99**, 10126-10131.
- Kambach, C., Walke, S. and Nagai, K. (1999a). Structure and assembly of the spliceosomal small nuclear ribonucleoprotein particles. *Curr. Opin. Struct. Biol.* **9**, 222-230.
- Kambach, C., Walke, S., Young, R., Avis, J. M., de la Fortelle, E., Raker, V. A., Luhrmann, R., Li, J. and Nagai, K. (1999b). Crystal structures of two Sm protein complexes and their implications for the assembly of the spliceosomal snRNPs. *Cell* **96**, 375-387.
- Kruhlak, M. J., Lever, M. A., Fischle, W., Verdin, E., Bazett-Jones, D. P. and Hendzel, M. J. (2000). Reduced mobility of the alternate splicing factor (ASF) through the nucleoplasm and steady state speckle compartments. *J. Cell Biol.* **150**, 41-51.
- Lefebvre, S., Burlet, P., Liu, Q., Bertrand, S., Clermont, O., Munnich, A., Dreyfuss, G. and Melki, J. (1997). Correlation between severity and SMN protein level in spinal muscular atrophy. *Nat. Genet.* **16**, 265-269.
- Lehmeier, T., Raker, V., Hermann, H. and Luhrmann, R. (1994). cDNA cloning of the Sm proteins D2 and D3 from human small nuclear ribonucleoproteins: evidence for a direct D1-D2 interaction. *Proc. Natl. Acad. Sci. USA* **91**, 12317-12321.
- Lerner, M. R. and Steitz, J. A. (1979). Antibodies to small nuclear RNAs complexed with proteins are produced by patients with systemic lupus erythematosus. *Proc. Natl. Acad. Sci. USA* **76**, 5495-5499.
- Liu, Q. and Dreyfuss, G. (1996). A novel nuclear structure containing the survival of motor neurons protein. *EMBO J.* **15**, 3555-3565.
- Lorson, C. L., Strasswimmer, J., Yao, J. M., Baleja, J. D., Hahnen, E., Wirth, B., Le, T., Burghes, A. H. and Androphy, E. J. (1998). SMN oligomerization defect correlates with spinal muscular atrophy severity. *Nat. Genet.* **19**, 63-66.
- Lührmann, R., Kastner, B. and Bach, M. (1990). Structure of spliceosomal snRNPs and their role in pre-mRNA splicing. *Biochim. Biophys. Acta* **1087**, 265-292.
- Lyon, C. E., Bohmann, K., Sleeman, J. and Lamond, A. I. (1997). Inhibition of protein dephosphorylation results in the accumulation of splicing snRNPs and coiled bodies within the nucleolus. *Exp. Cell Res.* **230**, 84-93.
- Malatesta, M., Zancanaro, C., Martin, T. E., Chan, E. K., Amalric, F., Lührmann, R., Vogel, P. and Fakan, S. (1994). Cytochemical and immunocytochemical characterization of nuclear bodies during hibernation. *Eur. J. Cell Biol.* **65**, 82-93.
- Massenet, S., Pellizzoni, L., Paushkin, S., Mattaj, I. W. and Dreyfuss, G. (2002). The SMN complex is associated with snRNPs throughout their cytoplasmic assembly pathway. *Mol. Cell. Biol.* **22**, 6533-6541.
- Matera, A. G. and Frey, M. R. (1998). Coiled bodies and gems: janus or gemini? *Am. J. Hum. Genet.* **63**, 317-321.
- Mattaj, I. W. (1986). Cap trimethylation of snRNA is cytoplasmic and dependent on U snRNP protein binding. *Cell* **46**, 905-911.
- Melki, J. (1997). Spinal muscular atrophy. *Curr. Opin. Neurol.* **10**, 381-385.
- Nagai, K. and Mattaj, I. W. (1994). RNA-protein interactions in the splicing snRNPs. In *RNA-Protein Interactions* (ed. K. Nagai and I. W. Mattaj), pp. 150-177. Oxford: Oxford University Press.
- Narayanan, U., Ospina, J. K., Frey, M. R., Hebert, M. D. and Matera, A. G. (2002). SMN, the spinal muscular atrophy protein, forms a pre-import snRNP complex with snurportin1 and importin beta. *Hum. Mol. Genet.* **11**, 1785-1795.
- Ochs, R. L., Stein, T. W. J. and Tan, E. M. (1994). Coiled bodies in the nucleolus of breast cancer cells. *J. Cell Sci.* **107**, 385-399.
- Paushkin, S., Gubitz, A. K., Massenet, S. and Dreyfuss, G. (2002). The SMN complex, an assemblyosome of ribonucleoproteins. *Curr. Opin. Cell Biol.* **14**, 305-312.
- Pearn, J. (1980). Classification of spinal muscular atrophies. *Lancet* **1**, 919-922.
- Pederson, T. (1998). The plurifunctional nucleolus. *Nucleic Acid Res.* **26**, 3871-3876.
- Pellizzoni, L., Charroux, B. and Dreyfuss, G. (1999). SMN mutants of spinal muscular atrophy patients are defective in binding to snRNP proteins. *Proc. Natl. Acad. Sci. USA* **96**, 11167-11172.
- Pellizzoni, L., Kataoka, N., Charroux, B. and Dreyfuss, G. (1998). A novel function for SMN, the spinal muscular atrophy disease gene product, in pre-mRNA splicing. *Cell* **95**, 615-624.
- Pettersson, I., Hinterberger, M., Mimori, T., Gottlieb, E. and Steitz, J. A. (1984). The structure of mammalian small nuclear ribonucleoproteins. Identification of multiple protein components reactive with anti-(U1) ribonucleoprotein and anti-Sm autoantibodies. *J. Biol. Chem.* **259**, 5907-5914.
- Phair, R. D. and Misteli, T. (2000). High mobility of proteins in the mammalian cell nucleus. *Nature* **404**, 604-609.
- Platani, M., Goldberg, I., Lamond, A. I. and Swedlow, J. R. (2002). Cajal body dynamics and association with chromatin are ATP-dependent. *Nat. Cell Biol.* **4**, 502-508.
- Platani, M., Goldberg, I., Swedlow, J. R. and Lamond, A. I. (2000). In vivo analysis of Cajal body movement, separation, and joining in live human cells. *J. Cell Biol.* **151**, 1561-1574.
- Raker, V. A., Plessel, G. and Luhrmann, R. (1996). The snRNP core assembly pathway: identification of stable core protein heteromeric complexes and an snRNP subcore particle in vitro. *EMBO J.* **15**, 2256-2269.
- Ramon-y-Cajal, S. (1903). Un sencillo metodo de coloracion selectiva del reticulo protoplasmico y sus efectos en los diversos organos nerviosos de vertebrados e invertebrados. *Trab. Lab. Invest. Biol.* **2**, 129-221.
- Raska, I., Andrade, L. E., Ochs, R. L., Chan, E. K., Chan, C. M., Roos, G. and Tan, E. M. (1991). Immunological and ultrastructural studies of the nuclear coiled body with autoimmune antibodies. *Exp. Cell Res.* **195**, 27-37.
- Sleeman, J., Lyon, C. E., Platani, M., Kreivi, J.-P. and Lamond, A. I. (1998). Dynamic interactions between splicing snRNPs, coiled bodies and nucleoli revealed using snRNP protein fusions to the green fluorescent protein. *Exp. Cell Res.* **243**, 290-304.
- Sleeman, J. E., Ajuh, P. and Lamond, A. I. (2001). snRNP protein expression enhances the formation of Cajal bodies containing p80-coilin and SMN. *J. Cell Sci.* **114**, 4407-4419.
- Sleeman, J. E. and Lamond, A. I. (1999a). Newly assembled snRNPs associate with coiled bodies before speckles, suggesting a nuclear snRNP maturation pathway. *Curr. Biol.* **9**, 1065-1074.
- Sleeman, J. E. and Lamond, A. I. (1999b). Nuclear organization of pre-mRNA splicing factors. *Curr. Opin. Cell Biol.* **11**, 372-377.
- Snaar, S., Wiesmeijer, K., Jochemsen, A. G., Tanke, H. J. and Dirks, R. W. (2000). Mutational analysis of fibrillarin and its mobility in living human cells. *J. Cell Biol.* **151**, 653-662.
- Talbot, K. and Davies, K. E. (2001). Spinal muscular atrophy. *Semin. Neurol.* **21**, 189-197.
- Terns, M. P. and Terns, R. M. (2001). Macromolecular complexes: SMN the master assembler. *Curr. Biol.* **11**, R862-864.
- Trinkle-Mulcahy, L., Sleeman, J. E. and Lamond, A. I. (2001). Dynamic targeting of protein phosphatase 1 within the nuclei of living mammalian cells. *J. Cell Sci.* **114**, 4219-4228.
- Tucker, K. E., Berciano, M. T., Jacobs, E. Y., LePage, D. F., Shpargel, K. B., Rossire, J. J., Chan, E. K., Lafarga, M., Conlon, R. A. and Matera, A. G. (2001). Residual Cajal bodies in coilin knockout mice fail to recruit Sm snRNPs and SMN, the spinal muscular atrophy gene product. *J. Cell Biol.* **154**, 293-307.
- Wang, J. and Dreyfuss, G. (2001). A cell system with targeted disruption of the SMN gene: functional conservation of the SMN protein and dependence of Gemin2 on SMN. *J. Biol. Chem.* **276**, 9599-9605.
- Yong, J., Pellizzoni, L. and Dreyfuss, G. (2002). Sequence-specific interaction of U1 snRNA with the SMN complex. *EMBO J.* **21**, 1188-1196.
- Young, P. J., Le, T. T., thi Man, N., Burghes, A. H. and Morris, G. E. (2000). The relationship between SMN, the spinal muscular atrophy protein, and nuclear coiled bodies in differentiated tissues and cultured cells. *Exp. Cell Res.* **256**, 365-374.